

Discontinuous molecular dynamics simulation study of polymer collapse

Sheldon B. Opps,^{a)} James M. Polson, and Nick Abou Risk

Department of Physics, University of Prince Edward Island, 550 University Avenue, Charlottetown, Prince Edward Island C1A 4P3, Canada

(Received 7 August 2006; accepted 12 October 2006; published online 16 November 2006)

Discontinuous molecular dynamics simulations were used to study the coil-globule transition of a polymer in an explicit solvent. Two different versions of the model were employed, which are differentiated by the nature of monomer-solvent, solvent-solvent, and nonbonded monomer-monomer interactions. For each case, a model parameter λ determines the degree of hydrophobicity of the monomers by controlling the degree of energy mismatch between the monomers and solvent particles. We consider a λ -driven coil-globule transition at constant temperature. The simulations are used to calculate average static structure factors, which are then used to determine the scaling exponents of the system in order to determine the θ -point values λ_θ separating the coil from the globule state. For each model we construct coil-globule phase diagrams in terms of λ and the particle density ρ . Additionally, we explore for each model the effects of varying the range of the attractive interactions on the phase boundary separating the coil and globule phases. The results are analyzed in terms of a simple Flory-type theory of the collapse transition.

© 2006 American Institute of Physics. [DOI: 10.1063/1.2388270]

I. INTRODUCTION

The coil-globule transition corresponds to the collapse of a single polymer chain in solution from an extended coil-like state to a compact globule state. This significant reduction in the average size of the polymer is driven by a change in the solvent conditions from “good” to “poor.” Although the coil-globule transition was first observed experimentally by Swislow *et al.*¹ and Nishio *et al.*² two decades ago, there remain a number of unresolved issues regarding the phase behavior and dynamics associated with polymer collapse. Thus, the study of polymer collapse remains an important area of research, especially in light of its connection with the early stages of protein folding. A recent review by Baysal and Karasz³ provides a thorough summary of the numerous studies carried out on the coil-globule transition.

There have been a number of different theoretical approaches to study this problem. The mean-field Flory-type⁴ theories are appealing in the sense that the free energy of the polymer-solvent system is expressed in terms of a *single* parameter characterizing the average size of the polymer. Variations of this method are still being developed⁵ and provide insight into simulation results.⁶ On the other hand, self-consistent integral equation theories provide a more detailed microscopic picture of polymer collapse and have been applied with some success to study the effects of solvent in this phenomenon.⁷⁻⁹ In Ref. 9 a new approach to solving these integral equations using transfer matrices has been developed. Another interesting approach has been developed by Taylor,¹⁰ which is based on distribution function theory. His results suggest an enhancement in effective monomer attractions with increasing monomer/solvent size ratio, implying the possibility of an entropy-driven coil-globule transition,

which has thus far only been observed in lattice systems.¹¹ More recently, Porter and Lipson¹² have used a continuum version of Born-Green-Yvon (BGY) theory to study the properties of square-well chain fluids. By explicitly incorporating density dependence into the intramolecular correlation function, they were able to examine the structural properties of a single short chain immersed in a square-well monomeric fluid of variable density.

Many simulation studies of polymer collapse have been performed for isolated chains, where solvent effects are implicitly built in to the model through effective pair interactions between monomers. Recently, explicit-solvent models have been employed to investigate the direct effects of the solvent on polymer phase behavior.^{6,11,13-21} In Ref. 21, the collapse dynamics of a polymer chain in solvent are probed using both molecular dynamics (with an explicit solvent) and Brownian dynamics (with an implicit solvent) simulations. Although the mechanisms of collapse appear similar for both simulation methods, with the development of sausage-like intermediate structures, the collapse process is smoother when an explicit solvent is used. The researchers suggest that in the Brownian dynamics simulation the polymer gets trapped in local minima and the equilibrium confirmation is often not reached. Hence, this is an important study demonstrating key differences in polymer collapse when explicit versus implicit solvent models are used. The Monte Carlo studies of Refs. 14 and 20 examine solvent screening effects in the context of polymer collapse and, hence, share a common focus with this paper.

The majority of the above mentioned articles utilize conventional molecular dynamics (MD) methods, whereby the equations of motion for the system are numerically solved at regularly spaced time intervals. An alternative method, referred to as *discontinuous molecular dynamics* (DMD) was developed by Alder and Wainwright²² to study hard-sphere

^{a)}Electronic mail: soppo@upepei.ca

systems, but has been generalized to study simple chemical systems,²³ polymers,^{24–26} complex protein structures,^{27,28} and semiflexible and rigid-body systems.^{29,30} The DMD method utilizes discontinuous potentials, whereby the forces acting between pairs of particles are impulsive and the equations of motion can be solved analytically from conservation equations. A typical simulation thus proceeds as a sequence of two-body “collisions,” where particles move with constant velocity in between collision events. In contrast to continuous-potential systems, the DMD approach allows structural and dynamical properties to be determined exactly (up to machine precision) and is significantly faster than conventional MD.^{31,32} Thus, the DMD method provides a better opportunity to study long-time phenomena.³³

In this paper, we study the coil-globule transition of a polymer chain in an explicit solvent using DMD simulations. We employ a model that is similar in spirit to that used in Ref. 6, although the present model is based on discontinuous potentials: the polymer is treated as a chain of monomers connected by stiff bonds, monomers and solvent particles have single-site interactions, and are of the same size. Two different versions of this model are examined, henceforth referred to as models I and II, which are discussed in detail in Sec. II. Numerous simulations were performed to accurately map out the coil-globule phase boundary, for both models, by varying both the solvent density and a hydrophobicity parameter λ . In addition, we have examined the effects of varying the range of the attractive interactions on the coil-globule transition. These results are then compared with a simple Flory-type theory in order to test certain approximations made in the theory and to explore the range of validity of these approximations.

The paper is organized as follows. Section II describes the two different polymer-solvent models employed in this study. Section III A outlines the procedure to accurately locate the coil-globule transition point, while Sec. III B provides the theory used to compare with the phase boundaries obtained from simulation. The basic “recipe” for performing DMD is then provided in Sec. IV A, and the simulation details are discussed in Sec. IV B. In Sec. V the results are presented and discussed, and in Sec. VI the key conclusions are summarized.

II. MODEL

We consider two polymer-solvent models in this study. For each model, the polymer is composed of hard spherical monomers of diameter σ immersed in a solvent composed of hard spherical particles of the same size. The two models are distinguished by the nature of the monomer-solvent (MS), solvent-solvent (SS), and nonbonded monomer-monomer (MM) interactions. In each model, some of the interactions have an attractive square well component in addition to the hard-core repulsive potential. The models are designed such that a tunable mismatch in the attractions controls the solvent quality, and thus the preferred state of the polymer.

In model I, the three nonbonded interactions have the form

$$\begin{aligned} U_{\text{MM}}(r) &= \infty, & r < \sigma \\ &= -\lambda\epsilon, & \sigma < r < f\sigma \\ &= 0, & r > f\sigma, \end{aligned} \quad (1)$$

$$\begin{aligned} U_{\text{MS}}(r) = U_{\text{SS}}(r) &= \infty, & r < \sigma \\ &= 0, & r > \sigma. \end{aligned}$$

Increasing the parameter λ thus increases the strength of the attraction between monomers, and thus will drive the polymer to collapse. Similarly, increasing the parameter f will increase the range of the attractive interactions between monomers and will thus tend to stabilize the collapsed state.

In model II, the interactions have the form

$$\begin{aligned} U_{\text{MS}}(r) &= \infty, & r < \sigma \\ &= -(1-\lambda)\epsilon, & \sigma < r < f\sigma \\ &= 0, & r > f\sigma, \end{aligned} \quad (2)$$

$$\begin{aligned} U_{\text{MM}}(r) = U_{\text{SS}}(r) &= \infty, & r < \sigma \\ &= -\epsilon, & \sigma < r < f\sigma \\ &= 0, & r > f\sigma. \end{aligned}$$

At $\lambda=0$, the attractions between the three pairs of particles are equal, and at intermediate to high solvent density this corresponds to good solvent conditions. However, as λ increases, the mismatch in the energies of the different interactions also increases. It becomes more energetically favorable for the monomers and solvent particles to phase separate, i.e., for the polymer to collapse. Thus, in this model as well, increasing λ also tends to drive collapse. Consequently, we refer to λ as the hydrophobicity parameter for both models.

In addition to the nonbonded interactions, adjacent monomers on the polymer chain are bonded together with the following interaction:

$$\begin{aligned} U_{\text{bond}}(r) &= 0, & |r - \sigma| < 0.1\sigma \\ &= \infty, & |r - \sigma| > 0.1\sigma. \end{aligned} \quad (3)$$

III. BACKGROUND THEORY

A. Locating the transition

In the limit of sufficiently long chain length, the physical size of a polymer obeys the well-known scaling relation

$$R \sim N^\nu, \quad (4)$$

where N is the number of statistical segments of the polymer and ν is the scaling exponent. An important example of polymer size is the average radius of gyration of the polymer \bar{R}_g defined as

$$\bar{R}_g \equiv \sqrt{\langle R_g^2 \rangle} \equiv \sqrt{\frac{1}{N} \sum_{n=1}^N \langle |\mathbf{R}_n - \langle \mathbf{R} \rangle|^2 \rangle}, \quad (5)$$

where \mathbf{R}_n is the position of monomer n , $\langle \mathbf{R} \rangle$ is the average monomer position, and where the angular brackets denote a

statistical averaging over polymer conformations. In the limit of large N , the scaling exponent assumes specific values, which characterize the state of the polymer chain. In good solvent conditions, the polymer is in the swollen coil state and $\nu \approx 0.5876$.³⁴⁻³⁶ Conversely, in poor solvent conditions, the polymer will be in the compact liquid-like globule state with $\nu = \frac{1}{3}$. Generally, the solvent conditions which determine the conformational state of a polymer in solution for a real physical system are determined by a complex interplay between the monomer-monomer, monomer-solvent, and solvent-solvent interactions. The solvent conditions can be changed upon variation of one or more system properties (e.g., temperature and/or pH), which can then trigger a transition between the coil and globule states. The transition will be manifested in a change in ν and a corresponding change in \bar{R}_g . It can be either continuous or first-order-like, depending on various properties such as the stiffness of the chain. The width of the transition decreases with increasing chain length. For the relatively short model polymers considered in this study, the transition is fairly broad. To locate the transition, we choose the so-called θ point, close to which the polymer behaves as though it were an ideal chain. Thus, the point where $\nu = \frac{1}{2}$ is chosen to define the location of the coil-globule transition. As stated in Ref. 6, this condition differs from the true θ point which is defined where the second virial coefficient vanishes. However, for finite-length chains, it is observed that the collapse transition is N dependent and occurs at slightly higher temperatures than the θ temperature. Although the θ point, the ideal-chain condition, and the collapse transition only converge in the thermodynamic limit ($N \rightarrow \infty$), in this study we will treat the $\nu = \frac{1}{2}$ condition as an operational definition of the coil-globule transition.

The static structure factor $S(\mathbf{k})$ of a polymer chain can be used to determine the conformational state of a polymer chain. Since the system is isotropic, the structure factor depends only on the magnitude of \mathbf{k} , and is given by

$$S(k) = \frac{1}{N} \sum_{m,n} \left\langle \frac{\sin[k|\mathbf{R}_m - \mathbf{R}_n|]}{k|\mathbf{R}_m - \mathbf{R}_n|} \right\rangle. \quad (6)$$

For the polymer chain considered in this study, the structure factor satisfies the relation

$$S(k) \propto k^{-1/\nu} \quad (7)$$

in the limit where $R_g^{-1} \ll k \ll \sigma^{-1}$, where σ is simultaneously the monomer size and the average bond length. Note that this condition is only satisfied for long chains, $N \gg 1$, for which $R_g \gg \sigma$. In the present case, where $N=30$, the chains are too short to rigorously satisfy the condition. On the other hand, as is evident in the sample calculated structure factor plotted on the log-log graph in Fig. 2, there is a linear regime apparent in the range defined by the less rigid criterion $R_g^{-1} \lesssim k \lesssim \sigma^{-1}$. In this study we use the slope m of this linear regime to calculate the scaling exponent according to $\nu = -1/m$. While we expect there to be non-negligible finite-size effects, the calculated coil-globule phase boundaries should display the general qualitative features present for longer-chain systems.

B. Comparing simulation results to theoretical predictions

Some understanding of the significance of the simulation results presented in this study can be gained from an analytical theoretical treatment of the polymer collapse transition. Here, we consider only the simple Flory-Huggins (FH) theory, in which the criterion for collapse is determined by the well-known Flory χ parameter, which in turn can be related to the parameters of the model polymer-solvent system.

First, we define the expansion coefficient α ,

$$\alpha^2 \equiv R_g^2 / \langle R_0^2 \rangle, \quad (8)$$

where $\langle R_0^2 \rangle$ is the average square radius of gyration of the corresponding ideal chain, i.e., in the absence of nonbonded interactions. The average expansion coefficient $\bar{\alpha} \equiv \sqrt{\langle \alpha^2 \rangle}$ has values in the range $\bar{\alpha} > 1$ for a swollen coil, $\bar{\alpha} < 1$ for a globule, and $\bar{\alpha} = 1$ under θ or ideal conditions, i.e., conditions under which the average chain size is equal to that of the ideal chain, for which nonbonded monomer-monomer or monomer-solvent interactions are lacking. Following the approach of Flory, the free energy of the polymer-solvent system is written as a function of this quantity,

$$F(\alpha) = F_{\text{el}}(\alpha) + F_{\text{int}}(\alpha), \quad (9)$$

where $F_{\text{el}}(\alpha)$ is the elastic free energy of the ideal chain and $F_{\text{int}}(\alpha)$ is the contribution to the free energy from particle interactions. An approximate expression for $F_{\text{el}}(\alpha)$ is given by³⁷

$$\begin{aligned} \beta F_{\text{el}}(\alpha) &= \frac{9}{4}(\alpha^{-2} + 2 \ln \alpha), \quad \alpha < 1 \\ &= (\pi^2/4)(\alpha^2 - 2 \ln \alpha), \quad \alpha > 1. \end{aligned} \quad (10)$$

In the vicinity of the θ point, the chain is sufficiently large such that the interaction term $F_{\text{int}}(\alpha)$ can be written as³⁸

$$\beta F_{\text{int}}(\alpha) = \left(\frac{B\sqrt{N}}{v} \right) \alpha^{-3} + \left(\frac{C}{v^2} \right) \alpha^{-6}, \quad (11)$$

where v is the excluded volume of each monomer. The first and second terms correspond to two- and three-body effects, respectively, arising from nonbonded interactions. Correspondingly, B and C refer to second- and third-order virial coefficients. Note that Eq. (11) is not expected to be valid in the regime of high compaction, i.e., in the globule state.

For a polymer-solvent system at liquid-like solvent densities, it is natural to employ the FH form of the coefficients B and C ,

$$B = v \left(\frac{1}{2} - \chi \right), \quad C = \frac{v^2}{6}. \quad (12)$$

In order to apply this theory to the simulation results of this study, we must choose a mapping between the off-lattice model employed in the simulations to the lattice model underlying the FH theory. For an off-lattice model, the simplest choice for the χ parameter is

$$\chi = \Delta \epsilon / k_B T, \quad (13)$$

where the energy mismatch $\Delta \epsilon$ is given by

$$\Delta\epsilon = \bar{\epsilon}_{MS} - \frac{1}{2}(\bar{\epsilon}_{SS} + \bar{\epsilon}_{MM}). \quad (14)$$

The energy terms are defined as

$$\bar{\epsilon}_{\alpha\beta} = \rho \int_0^\infty dr 4\pi r^2 g_{\alpha\beta}(r) u_{\alpha\beta}(r), \quad (15)$$

where $g_{\alpha\beta}(r)$ is the radial distribution function between particles of type α and β . We employ the simple random mixing approximation, whereby $g_{MM}(r) = g_{MS}(r) = g_{SS}(r) \equiv g(r)$, i.e., all three radial distribution functions are equal. For the models defined in Sec. II, the expression for χ can then be written as

$$\chi = \frac{2\pi G \lambda \epsilon \rho}{k_B T} \int_\sigma^{f\sigma} dr r^2 g(r), \quad (16)$$

where G is a numeric factor with a value of $G=1$ for model I and $G=2$ for model II.

In order to calculate χ , the form of the radial distribution function $g(r)$ must be chosen. We use the value for $g(r)$ calculated using the solution to the Ornstein-Zernicke equation with the Percus-Yevick approximation for a suitable reference system. In the case of model I, we observe that the transition occurs for relatively small values of $\lambda\epsilon/k_B T$, i.e., for relatively weak monomer-monomer attraction, in which case the interaction is effectively close to a hard-sphere interaction. Since, in addition, the monomer-solvent and solvent-solvent interactions are of hard-sphere type, we choose a hard-sphere reference system for particles with diameter σ . In the case of model II, the transition also typically occurs for small values of λ . In this case, it means that the depth of the monomer-solvent attractive square well is close to ϵ , the depth of the monomer-monomer and solvent-solvent square well. Consequently, an appropriate reference system to use to estimate $g(r)$ is that of particles interacting with hard spherical cores of diameter σ and attractive square wells of depth ϵ and of range $f\sigma$.

The collapse transition considered in this study is driven by variation of the hydrophobicity parameter λ defined for each of the models in Eqs. (1) and (2). Thus, in the context of the present theory, variation of λ controls χ , and thus B , by changing the energy mismatch factor $\Delta\epsilon$. At a certain value of the hydrophobicity parameter λ_θ , the θ condition $\bar{\alpha}=1$, or equivalently $\nu=\frac{1}{2}$, is satisfied. The theoretical prediction for λ_θ is obtained as follows. For a range of λ , we calculate χ in Eq. (16) using the appropriate form of $g(r)$, as discussed above. This is used to calculate the second virial coefficient in Eq. (12), which, in turn is used to find the form of $F_{\text{int}}(\alpha)$ in Eq. (11). Using the form for the elastic free energy of the ideal chain in Eq. (10), the full free energy $F(\alpha)$ is then determined. Given that the probability that the polymer assumes a conformation of size α is proportional to $\exp(-F(\alpha)/k_B T)$, $\bar{\alpha}$ may then be determined from the following expression:

$$\bar{\alpha}^2 = \langle \alpha^2 \rangle = \frac{\int_0^\infty d\alpha \alpha^2 \exp(-\beta F(\alpha))}{\int_0^\infty d\alpha \exp(-\beta F(\alpha))}. \quad (17)$$

The θ point can then be determined by tuning the parameter λ until we find the value λ_θ that yields $\bar{\alpha}=1$.

Finally, it is worth noting the limitations of the Flory-type theory presented above, in particular, the enthalpic form of χ assumed in Eq. (13). From computer simulation studies of polymer solutions, it is known that polymers of athermal polymer-solvent model systems decrease in physical size with increasing solvent density. The origin of this effect is purely entropic in nature and is usually described theoretically in terms of ‘‘solvation potentials,’’ effective attractive pair potentials between monomers which are mediated by the solvent. A theoretical description of this entropic effect has been provided in various integral equation theories. However, inclusion of such entropic effects into the theory for the type of model employed here is difficult and beyond the scope of the present work. Consequently, the theory cannot provide an accurate prediction, for example, of the dependence of the transition point on the solvent density. This dependence will be strongly influenced by entropic effects.

IV. DMD SIMULATION METHOD

A. Background

We utilize the DMD method, whereby the dynamics of the system are solved analytically so that the positions and velocities of the particles are determined exactly. Since the potentials are discontinuous, the forces between particles are impulsive and only act at specific moments of time. Hence, particles move with uniform velocity in between impulsive events. These ‘‘collision events’’ are determined by

$$|\mathbf{r}_{ij}(t_0 + t_{ij})| = |\mathbf{r}_0(t_0) + \mathbf{v}_{ij}t_{ij}| = \sigma, \quad (18)$$

where t_{ij} is the time for which particles i and j are at a separation equal to σ corresponding to a discontinuity in the potential. Solving for this collision time yields

$$t_{ij} = \frac{-b_{ij} \pm \sqrt{b_{ij}^2 - v_{ij}^2(r_{ij}^2 - \sigma^2)}}{v_{ij}^2}, \quad (19)$$

where $b_{ij} = \mathbf{r}_{ij} \cdot \mathbf{v}_{ij}$. Upon ‘‘colliding,’’ the velocities of the particles are altered. The nature of this change depends on whether the potential energy U changes upon collision or remains the same.

(1) If $\delta U \neq 0$,

$$\delta \mathbf{v}_i = \frac{\mathbf{r}_{ij} \mu b_{ij}}{\sigma^2 m_i} \left[\sqrt{1.0 - \frac{2.0 \delta U \sigma^2}{\mu b_{ij}^2}} - 1.0 \right], \quad (20)$$

$$\delta \mathbf{v}_j = -\delta \mathbf{v}_i,$$

where μ is the reduced mass of the two particles involved in the collision.

(2) If $\delta U = 0$,

$$\delta \mathbf{v}_i = \frac{-2.0 \mu \mathbf{r}_{ij} b_{ij}}{m_i \sigma^2}, \quad (21)$$

$$\delta \mathbf{v}_j = -\delta \mathbf{v}_i.$$

These ‘‘collision rules’’ are derived from the equations for conservation of momentum and energy.

In addition to the core procedures described above, we em-

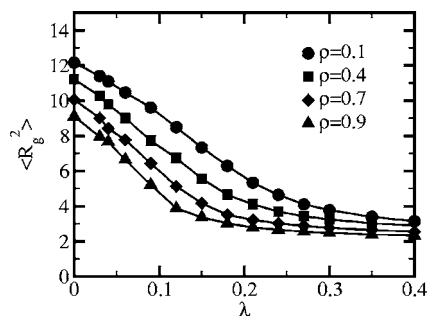


FIG. 1. $\langle R_g^2 \rangle$ vs λ for model I for a polymer of length $N=30$ in solvents of various densities at $T=1.0$. The range of the monomer-monomer attractive square well is $f=2.0$ for the data shown.

ploy three standard techniques to improve the efficiency of the DMD algorithm: (1) subcells and link lists,³⁹ (2) binary tree event scheduling,⁴⁰ and (3) local clocks.⁴¹

B. Simulation details

Simulations were performed on the Glacier cluster, which is part of the WestGrid computational facility located in Western Canada. Glacier is an IBM eServer cluster consisting of 840 computational nodes (each with dual 3.0 GHz Intel Xeon processors) connected via a gigE network. A typical simulation required on the order of 12–40 h of CPU time to execute. We used a cubic simulation box with periodic boundary conditions.

1. Simulation setup

The monomers and solvent particles were initially placed on a cubic lattice, where the polymer was inserted along one face of the box with alternating parallel segments. Most simulations were performed with polymers of length $N=30$ immersed in a bath of N_s particles, such that the total number of particles was $N+N_s=1000$. However, polymer lengths of $N=30$, 40, and 50 were also employed to examine finite-size effects. All of the results are expressed in reduced units, unless otherwise specified.

2. Thermalization and averages

A typical simulation required on the order of a few hundred reduced time units to equilibrate, depending on the model, the range of the interaction potential, and the density. During equilibration, velocity rescaling was used to reach the target temperature, which for model I was $T=1.0$ and for model II was $T=2.0$.

Average static structure factors were calculated from relatively long production runs, on the order of $\Delta t = 25\,000$ – $350\,000$, in order to achieve good statistics. The average structure factor was then used to determine the scaling exponent ν . To obtain sufficient values of ν in order to accurately determine λ_θ , 9–11 simulations were performed at different values of λ . 9–10 sets of these simulations, for various values of the density, were performed in order to map out a phase diagram. This procedure was repeated for different values of f , the parameter controlling the range of the intermolecular potential, for each model.

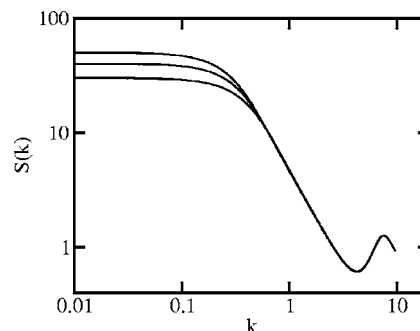


FIG. 2. Structure factor functions $S(k)$ for polymers of length $N=50$, 40, and 30, from top to bottom. These data were calculated for the model I system at a density of $\rho=0.5$, a temperature of $T=1.0$, and at $\lambda=0$.

V. RESULTS AND DISCUSSION

Figure 1 shows the average square radius of gyration, $\langle R_g^2 \rangle$, as a function of the hydrophobicity parameter λ for the model I polymer-solvent system at a temperature $T=1.0$ for four different solvent densities. Recall that λ is the depth of the square well of the interaction potential between non-bonded monomers. As expected, an increase in this attraction causes the polymer to collapse. At $\lambda=0$, there is no monomer-monomer attraction; thus, the system is simply a hard-sphere chain in a hard sphere solvent. At this point, the polymer assumes its largest size as a swollen coil. By $\lambda \approx 0.35$, the polymer has collapsed to a globule for the full range of solvent densities considered.

There are two noteworthy trends with regard to variations of $\langle R_g^2 \rangle$ with the solvent density ρ . First, at any given value of λ , $\langle R_g^2 \rangle$ decreases with increasing ρ . Second, the polymer collapses at lower values λ for higher ρ . To better quantify the second feature, we calculate the θ point by determining the variation of the scaling exponent ν with λ . Figure 2 shows typical structure factors plotted on a log-log graph for polymers of lengths $N=30$, 40, and 50. In the linear portion of the curves, the structure factor scales as $S(k) \propto k^{-1/\nu}$. Fitting this linear part of the curve, one obtains the slope and, hence, the exponent ν . Figure 3 shows the variation of ν with λ . Consistent with the results in Fig. 1 and in light of the scaling relation (4), ν decreases with increasing λ . At $\lambda=0$, ν is close to the good solvent theoretical value of

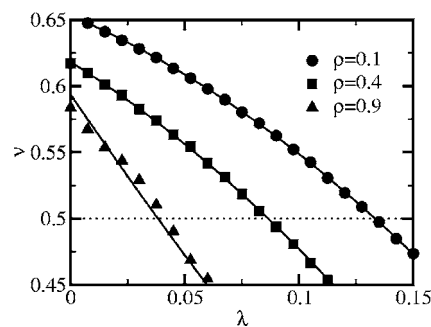


FIG. 3. Polymer scaling exponents ν vs λ for the model I polymer solvent system at three different solvent densities. For the data shown, the polymer had a length of $N=30$, the range of the monomer-monomer potential square well was $f=2.0$, and the temperature was $T=1.0$. The solid lines show fits to a quadratic polynomial. The intersection of the fitted curves with the $\nu = \frac{1}{2}$ line determines the approximate values of λ_θ .

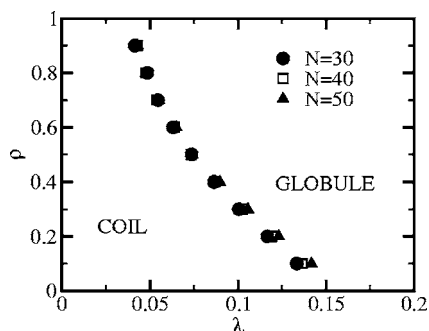


FIG. 4. Model I phase diagram for three different polymer lengths. For each case, the range of the monomer-monomer attraction is $f=2.0$.

$\approx \frac{3}{5}$. In order to minimize the effects of statistical fluctuations, the data were fitted to a function which is then used for interpolation. The solid curves in the figure show a fit to a quadratic function, which appears to provide a sufficient fit. The intersection points of these curves with the $\nu = \frac{1}{2}$ yield the λ_θ . Again, consistent with the results of Fig. 1, the θ -point values increase with increasing density.

Figure 4 shows a phase diagram for the model I system for chain lengths of $N=30, 40$, and 50 . In each case, there is a monotonic decrease in λ_θ with increasing solvent density. On the other hand, there is very little effect on the phase boundary on increasing the chain length. There appears to be a slight increase in λ_θ with increasing N at low solvent density, and no discernible effect at high density.

The origin of the stabilization of the globule state with increasing solvent density, evident in Figs. 1, 3, and 4, must be entropic in nature. In the absence of a solvent, the polymer collapse transition is controlled by two competing driving forces. First, the conformational entropy of the chain with monomer-monomer excluded volume interactions favors a swollen coil state. Second, the attractions between monomers provide an energetic driving force towards the collapsed globule state. The parameter λ determines the strength of the latter with respect to the former. Increasing λ increases the strength of monomer attraction which eventually compensates for the loss in conformational entropy and leads to collapse. The presence of a solvent changes the nature of this balance. Solvent particles interact with monomers and other solvent particles only with hard-core interactions. Consequently, the presence of the solvent for any polymer configuration corresponding to some value of the expansion coefficient α does not change the energy of the system. On the other hand, any polymer conformation will impose restrictions on the possible arrangements of solvent particles around the polymer. Since the polymer size decreases with ρ , it is clear that the solvent entropy increases as the polymer size decreases, and thus favors the globule state. In the context of various integral equation theories of polymers in solution, this effect is usually described in terms of a solvation potential, that is, a solvent-mediated effective pair potential between monomers. Consistent with the results of this and other studies, this solvent-induced monomer-monomer attraction increases with increasing solvent density. The solvation potential is similar in nature to so-called depletion forces in colloid-polymer mixtures.

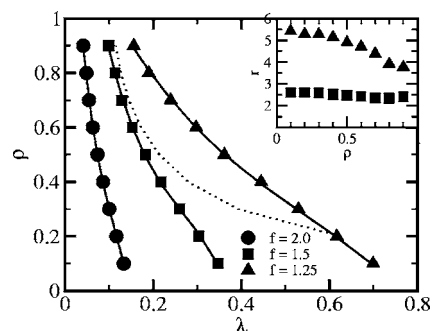


FIG. 5. Phase diagrams for the model I system with a polymer of length $N=30$ at a temperature of $T=1.0$. The coil-globule phase boundaries for monomer-monomer square-well attraction ranges of $f=2.0, f=1.5$, and $f=1.25$ are shown. The coil and globule regions are to the left and to the right of the phase boundaries, respectively. The dotted line shows the prediction based on the theory described in Sec. III B. The inset shows the variation with solvent density ρ of the ratio r of λ_θ of $f=1.5$ to $f=2.0$ (squares) and of $f=1.25$ to $f=2.0$ (triangles).

Figure 5 shows coil-globule phase boundaries for model I for polymers with three different ranges of monomer-monomer attraction. While the shapes of the curves are all similar, there is a marked shift in the boundary towards higher λ as the range f decreases. The origin of this shift is straightforward. As the range of monomer-monomer attraction decreases, a deeper square well is required to provide a sufficient driving force for the chain to collapse. The dotted line in the graph is the prediction from theory for the intermediate value of $f=1.5$. The theory performs well at sufficiently high solvent densities, but the stability of the coil phase is over predicted at lower densities. Discrepancies between theory and simulation at lower densities are anticipated, since the Flory-theory presented in Sec. III B was developed for a polymer-solvent system at *liquid-like* densities. The inset shows a plot of the ratio r of the λ_θ values for $f=1.5$ to $f=2.0$ (squares) and of $f=1.25$ to $f=2.0$ (triangles). The first ratio is almost constant, with only a slight decrease with increasing solvent density. The second ratio shows a more pronounced decrease with solvent density. Our interpretation of this behavior is as follows. At low ρ the only significant drive to chain collapse comes from the attraction between monomers. On the other hand, at high ρ , the entropic effect of solvent-induced effective attraction between monomers also contributes to driving the chain to collapse. Assuming this effective interaction is approximately independent of f , it will make a larger relative contribution in driving the chain to collapse. Consequently, the attractive well need not be deepened by as great a factor in order for collapse to occur.

Figure 6 shows a plot of λ_θ versus the monomer-monomer square-well range for model I for a polymer in a solvent at a high density of $\rho=0.9$. Consistent with the data in Fig. 4, λ_θ increases monotonically with decreasing range. As explained above, this follows from the fact that the attractive well must be deepened as its range is reduced in order to provide the driving force needed for chain collapse. The dependence of λ_θ on ρ is roughly linear over the range $f \in [1.3, 2.0]$. For $f \leq 1.3$, it rises steeply, consistent with the requirement that $\lambda_\theta \rightarrow \infty$ as $f \rightarrow 1$; that is, the well depth in

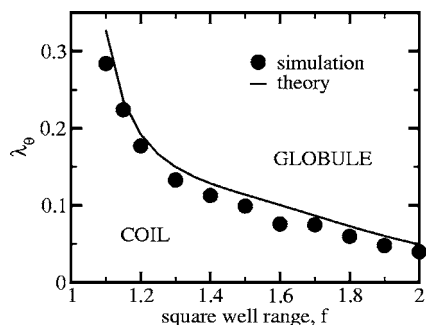


FIG. 6. λ_θ vs square well range f for model I for a polymer of length $N=30$ in a solvent of density $\rho=0.9$ and at a temperature of $T=1.0$. The solid curve shows a prediction using the theory in Sec. III B.

principle needs to become infinitely deep as the well width (which is $f-1$) becomes vanishingly small. Also shown in the graph is the prediction from the theory presented in Sec. III B. Given the number of approximations employed, the theory gives a reasonably good prediction of the f dependence of λ_θ over the full range of f considered, i.e., $f \in [1.1, 2.0]$. The theory consistently overestimates λ_θ by about 17% on average.

The methods used to calculate the coil-globule transition point for model I were also used for model II. As for model I, simulations were carried out for chains of length $N=30$ in a solvent with a density in the range $\rho \in [0.1, 0.9]$ and for square-well ranges $f \in [1.1, 2.0]$. Note that the range of attraction for this model is the same for all three pair potentials, as is evident in Eq. (2). All simulations were carried out at $T=2.0$, a higher temperature than that used for model I, in order to ensure that the solvent remained in a fluid state for all densities considered.

Figure 7 shows the phase diagram for model II for square-well ranges of $f=1.5, 1.7, 1.8$, and 2.0 . The phase boundaries are fundamentally different in shape from those of model I. With the exception of $f=2.0$, at high ρ , λ_θ initially increases with decreasing density. Thus, as in model I, the globule state becomes less stable as the solvent density decreases. However, at intermediate densities, the trend is reversed, and the globule state becomes more stable as the

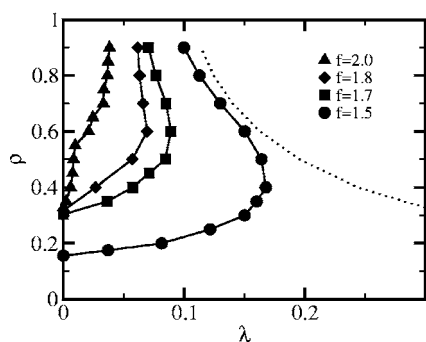


FIG. 7. Coil-globule transition boundaries for the model II system with a polymer of length $N=30$ at a temperature of $T=2.0$. The range of attraction of the square well f is the same for all three pairs of interactions. Phase boundaries for ranges of $f=2.0, 1.8, 1.7$, and 1.5 are shown. In each case, the coil and globule regions are to the left and to the right of the phase boundaries, respectively. The dotted line shows the prediction based on the theory described in Sec. III B

density decreases. Below some critical density, which depends on the range of the attraction, the globule state is stable over the whole range of λ . The shape of the phase boundary corresponds to reentrant phase behavior: for certain values of the hydrophobicity parameter λ (e.g., $\lambda=1.25$ for $f=1.5$) the polymer changes from a globule to a coil and back to a globule upon an increase in ρ .

To understand the significance of the model II phase diagrams, it is useful to consider first the isolated chain. Nonbonded monomers of the chain interact with an attractive square well of fixed depth. The temperature $T=2.0$ considered is sufficiently low that the monomer-monomer attractions overcome the loss in configurational entropy and stabilize the globule state. Since the intrachain attractions are independent of λ , this is the stable state at $\rho=0$ for the full range of λ . For finite solvent density, these intrachain attractions can become screened by the solvent particles. In the case of $\lambda=0$, the screening is most effective. This corresponds to a system where the monomer-solvent potential square wells are the same depth as those of the monomer-monomer and solvent-solvent interactions. The screening arises from the fact that a low value of the energy of the system can be achieved by increasing the number of monomer-solvent interactions. As the density increases, a gain in potential energy resulting from fewer monomer-monomer contacts for a larger average chain size is offset by the decrease in potential energy from an increased number of monomer-solvent contacts. Consequently, it is expected that as the solvent density increases, the energetic favorability for the globule state will diminish, the conformational entropy of the chain will increase, and the coil state will be stabilized. The coil will be the preferred state for $\lambda=0$ over a wide range of ρ . As λ increases, the depth of the monomer-solvent potential square well decreases. This diminishes the ability for the solvent to screen the intrachain attractions, since a monomer-solvent contact then has a higher energy than a monomer-monomer contact or a solvent-solvent contact. Thus, the coil state becomes increasingly unstable with respect to the globule state with increasing λ , and collapse eventually occurs. From these arguments, we therefore expect that the coil state will be stable only at sufficiently low λ and at moderate to high ρ , precisely the behavior seen in the figure.

The reentrant behavior in the phase diagram arises from a competition between screening and entropic effects of the solvent. As described earlier, the solvent entropy increases when the polymer size decreases, i.e., there are more configurations of solvent particles available for smaller α . Consequently, this acts to stabilize the globule phase. This solvent entropy effect strengthens with increasing solvent density. Thus, at sufficiently high ρ , it is expected that this effect could override the screening effect described earlier and lead to an increase in the stability of the globule state as ρ increases. This is exactly what is observed, at least, for systems with sufficiently small f . It is noteworthy that this feature diminishes as the range of attraction increases, until, at $f=2.0$, it is entirely absent. The theoretical predictions are also presented in Fig. 7 for $f=1.5$. There is good agreement between the theory and simulation results at higher densities,

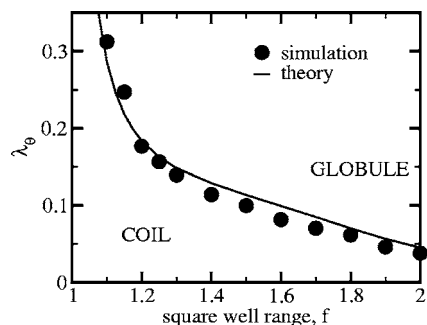


FIG. 8. λ_θ vs square well range f for model II for a polymer of length $N=30$ in a solvent of density $\rho=0.9$ and at a temperature of $T=2.0$. The solid curve shows a prediction using the theory in Sec. III B.

as was also seen with model I. However, the theory does not perform well at lower densities, where screening effects play a dominant role, and is thus unable to capture the reentrant behavior as observed with the simulations. The departure of the theory from simulations at lower densities is again anticipated, since the features responsible for screening effects of the solvent were not built into the theory.

Figure 8 shows λ_θ versus f for the model II system at a density of $\rho=0.9$. Consistent with the data in Fig. 7, the values decrease monotonically with increasing f . Also shown in the figure is the prediction for λ_θ using the theory described in Sec. III B. The agreement between the theory and simulation results is generally good. The observed decrease in λ_θ with f for this model can be understood relatively easily in the context of the theory. The f dependence of the free energy appears in the integral in the expression for χ in Eq. (16). Recall that, for model II, we chose $g(r)$ to be that obtained from the solution to the Ornstein-Zernicke equation using the Percus-Yevick approximation for a system of hard spheres of diameter σ with attractive square wells of range $f\sigma$ and depth ϵ . Consequently, the f dependence arises from the choice of $g(r)$, as well as in the upper limit of the integral in the equation. In practice, however, in our calculations we observe that the variation of this choice of $g(r)$ with f is sufficiently weak such that the running integral of $r^2g(r)$ is almost independent of f . Consequently, the f dependence of χ is mostly determined by the upper limit on the integral, $f\sigma$, which clearly leads to a monotonic increase in χ with f . From Eq. (12), this implies a decrease in the second virial coefficient B with increasing f . As decreasing B implies an increase in the effective attraction between monomers, this causes the globule state to become increasingly stable for arbitrary λ , and, thus, to a decrease in λ_θ with f .

The phase diagrams for the model I and model II systems are qualitatively similar to those for two comparable models employed in the MD study of Ref. 6. In that study, model B was a continuous-potential model based on the Lennard-Jones interaction which is comparable to model I here. Specifically, monomer-solvent and solvent-solvent interactions were solely repulsive, while monomer-monomer interactions had a attractive well whose depth was given by the hydrophobicity parameter λ . Likewise, model A of that study is comparable to model II here. As in the phase diagram for model I, the phase boundary of model B of Ref. 6

shifted to lower λ for increasing solvent density. Likewise, some of the generic behaviors of the phase boundaries observed for model II are also seen in the model A phase diagram of Ref. 6. Specifically, the coil state is stable only for moderate to high ρ and sufficiently low λ in each case. Note, however, that the reentrant behavior observed for certain values of the range, f , in Fig. 7, is a feature that was not observed in the corresponding phase diagram of Ref. 6. In that study, a truncated and shifted Lennard-Jones potential was used, with a cutoff distance of $r_c=3\sigma$, and hence the range of the attractive interactions was fixed. For continuous Lennard-Jones-type potentials, the range of the attractions cannot be varied without affecting other key aspects of the potential, including the depth of the potential. Thus one cannot, in a transparent fashion, independently study the effects of varying the range of the attractive interactions on the coil-globule phase boundary.

The results presented in this study are consistent with some recent Monte Carlo^{14,20} (MC) studies, where solvent screening effects have also been explored. In Ref. 14, a Lennard-Jones system consisting of a single-chain in a monomeric solvent was studied over a range of densities to examine the phase behavior that occur in a supercritical fluid. They observe that the coil-globule transition temperature is depressed relative to its vacuum value due to the presence of solvent near the chain which impedes collapse by excluding close intrachain contacts. Similar findings were made in Ref. 20, where configurational-bias MC simulations were performed for a single-chain composed of hard spheres and/or square-well spheres in a square-well solvent. Note that both of these studies were performed for shorter-length chains and at lower densities than investigated in the present study.

VI. CONCLUSIONS

In this paper DMD simulations were performed to study the coil-globule transition of a polymer in an explicit solvent. Two different versions of the model were employed, which differ by the nature of the monomer-monomer, solvent-solvent, and monomer-solvent interactions. For both models, we have mapped out the coil-globule phase diagrams in terms of a hydrophobicity parameter λ and the solvent density ρ . Additionally, we have probed the effects of varying the attractive interactions on the phase boundary separating coil and globule phases. These results are compared with a simple Flory-type theory of the collapse transition.

For model I, where solvent particles interact with monomers and other solvent particles with only hard-core interactions, the energetics of the system are governed by monomer-monomer interactions. Hence, at a given density, increasing λ enhances the attractions between monomers and causes the polymer to collapse. Decreasing the range of the monomer-monomer attraction stabilizes the coil phase, since a deeper square well is required to drive the chain to collapse. At fixed λ , increasing the density also causes the polymer size to decrease. This entropic effect is described by solvent-induced effective attraction between monomers which, at higher densities, increasingly favors chain collapse.

Such entropic effects, at higher densities, make a greater relative contribution in driving the chain to collapse as the range of the attractive interactions is decreased.

For model II, the monomer-monomer and solvent-solvent interactions are described by square-well potentials of equal and fixed depths, while the depth of the monomer-solvent square potential is varied. At low densities, the intrachain attractions dominate the energetics of the polymer and the globule phase remains stable at all values of λ . At intermediate densities and low values of λ , the intrachain attractions are screened by the solvent particles and the coil phase is stabilized. Increasing λ decreases this screening effect, as the monomer-solvent interactions are weakened. At sufficiently high densities and low values of f , one observes reentrant behavior, where the globule phase once again becomes the more stable phase. This reentrance is due to a competition between solvent entropy and screening effects which become increasingly important at higher densities.

We find good agreement between the off-lattice Flory theory and the simulation results, except at lower densities where the region of stability for the coil phase is over predicted. Furthermore, this theory is unable to reproduce the reentrant behavior discussed above, since the solvent screening effects are not built into the theory.

Although the potentials used in this study only roughly approximate those used in Ref. 6, the overall phase behavior for both models is faithfully replicated. Furthermore, by using discontinuous potentials one may separate out purely entropic effects, as seen with model I, whereas with the soft-repulsive potentials used in Ref. 6, such a separation cannot be made as energetic contributions exist even for $\lambda=0$. In addition, the ability to tune the range of the attractive interactions in order to probe the effects on the coil-globule phase transition is a feature of this study which cannot be transparently achieved with the use of continuous, Lennard-Jones (LJ)-type potentials.

In future work on isolated polymer chains in explicit solvent, we will examine entropic effects of the solvent caused by a mismatch in the solvent/monomer size ratio. To complement these simulation studies, more advanced theoretical approaches will be invoked, including the polymer reference interaction site model (PRISM) theory and scaled particle theory (SPT).

ACKNOWLEDGMENTS

This work has been supported by the National Research Council of Canada (NSERC) and by the Canadian Foundation for Innovation (CFI). We are grateful to the Advanced

Computational Research Laboratory (ACRL) at the University of New Brunswick and to WestGrid for use of their computational facilities.

- ¹G. Swislow, S.-T. Sun, I. Nishio, and T. Tanaka, *Phys. Rev. Lett.* **44**, 796 (1980).
- ²I. Nishio, S.-T. Sun, G. Swislow, and T. Tanaka, *Nature (London)* **281**, 208 (1979).
- ³B. M. Baysal and F. E. Karasz, *Macromol. Theory Simul.* **12**, 627 (2003).
- ⁴P. J. Flory, *Principles of Polymer Chemistry* (Cornell University Press, Ithaca, NY, 1953).
- ⁵C. P. Lowe and M. W. Dreischor, *J. Chem. Phys.* **122**, 084905 (2005).
- ⁶J. M. Polson and N. E. Moore, *J. Chem. Phys.* **122**, 024905 (2005).
- ⁷H. H. Gan and B. C. Eu, *J. Chem. Phys.* **109**, 2011 (1998).
- ⁸H. H. Gan and B. C. Eu, *J. Chem. Phys.* **110**, 3235 (1999).
- ⁹L. Livadaru and A. Kovalenko, *J. Chem. Phys.* **109**, 10631 (2005).
- ¹⁰M. P. Taylor, *J. Chem. Phys.* **121**, 10757 (2004).
- ¹¹M. Dijkstra, D. Frenkel, and J.-P. Hansen, *J. Chem. Phys.* **101**, 3179 (1994).
- ¹²J. A. Porter and J. E. G. Lipson, *J. Chem. Phys.* **122**, 094906 (2005).
- ¹³M. Dijkstra and D. Frenkel, *Phys. Rev. Lett.* **72**, 298 (1994).
- ¹⁴G. Luná-Barcenas, J. C. Meredith, I. C. Sanchez, K. P. Johnston, D. G. Gromov, and J. J. de Pablo, *J. Chem. Phys.* **107**, 10782 (1997).
- ¹⁵V. V. Vasilevskaya, P. G. Khalatur, and A. R. Khokhlov, *J. Chem. Phys.* **109**, 5108 (1998).
- ¹⁶J. M. Polson, *Phys. Rev. E* **60**, 3429 (1999).
- ¹⁷J. M. Polson and M. J. Zuckermann, *J. Chem. Phys.* **113**, 1283 (2000).
- ¹⁸J. M. Polson and M. J. Zuckermann, *J. Chem. Phys.* **116**, 7244 (2002).
- ¹⁹C. F. Abrams, N. K. Lee, and S. P. Obukhov, *Europhys. Lett.* **59**, 391 (2002).
- ²⁰M. Lísal and I. Nezbeda, *J. Chem. Phys.* **119**, 4026 (2003).
- ²¹R. Chang and A. Yethiraj, *J. Chem. Phys.* **114**, 7688 (2001).
- ²²B. J. Alder and T. E. Wainwright, *J. Chem. Phys.* **31**, 459 (1959).
- ²³G. A. Chapela, S. E. Martínez-Casas, and J. Alejandre, *Mol. Phys.* **53**, 139 (1984).
- ²⁴Y. Zhou, C. K. Hall, and M. Karplus, *Phys. Rev. Lett.* **77**, 2822 (1996).
- ²⁵D. C. Rapaport, *Phys. Rev. E* **68**, 041801 (2003).
- ²⁶Z. Li and C. K. Hall, *Langmuir* **21**, 7579 (2005).
- ²⁷Y. Zhou and M. Karplus, *Proc. Natl. Acad. Sci. U.S.A.* **94**, 14429 (1997).
- ²⁸Y. Zhou and M. Karplus, *J. Mol. Biol.* **293**, 917 (1999).
- ²⁹G. Ciccotti and G. Kalibaeva, *J. Stat. Phys.* **115**, 701 (2004).
- ³⁰L. H. de la Peña, R. van Zon, J. Schofield, and S. B. Opps, e-print cond-mat/0607527.
- ³¹J. Liu, T. L. B. II, and J. J. R. Elliott, *Ind. Eng. Chem. Res.* **33**, 957 (1994).
- ³²L. H. de la Peña, R. van Zon, J. Schofield, and S. B. Opps, e-print cond-mat/0607528.
- ³³S. Smith, C. Hall, and B. Freeman, *J. Comput. Phys.* **134**, 16 (1997).
- ³⁴H.-P. Hsu, W. Nadler, and P. Grassberger, *Macromolecules* **37**, 4658 (2004).
- ³⁵T. Prellberg, *J. Phys. A* **34**, L599 (2001).
- ³⁶P. Belohorec and B. G. Nickel, University of Guelph Report, 1997 (unpublished).
- ³⁷T. M. Birshtein and V. A. Pryamitsyn, *Macromolecules* **24**, 1554 (1991).
- ³⁸A. Y. Grosberg and A. R. Khokhlov, *Statistical Physics of Macromolecules* (American Institute of Physics, Woodbury, NY, 1994).
- ³⁹M. P. Allen and D. J. Tildesley, *Computer Simulation of Liquids* (Clarendon, New York, NY, 1987).
- ⁴⁰D. C. Rapaport, *J. Comput. Phys.* **34**, 184 (1980).
- ⁴¹J. J. Erpenbeck and W. W. Wood, in *Statistical Mechanics*, edited by B. J. Berne (Plenum, New York, 1977), Pt. B.

The Journal of Chemical Physics is copyrighted by the American Institute of Physics (AIP). Redistribution of journal material is subject to the AIP online journal license and/or AIP copyright. For more information, see <http://ojps.aip.org/jcpo/jcpcr/jsp>